

# Measurement of PSD Parameters and Proton Quenching in Organic Liquid Scintillators at the MLL \*

V. Zimmer, J. Winter, C. Ciemniak, L. Oberauer, W. Potzel, L. Prade, J. Scherzinger,  
R. Strauss, S. Schönert, S. Wawoczny  
Technische Universität München, 85748 Garching, Germany

## Introduction

The characterisation of proton recoil signals in organic liquid scintillators is crucial to understand both signal and backgrounds in rare event neutrino experiments like the proposed next-generation neutrino experiments LENA [1] and JUNO [2] and currently running neutrino detectors like Double Chooz [3] and Borexino [4].

LENA and JUNO are two projects aiming for very large liquid scintillator targets in the 20 to 50 kton range. The feasibility of LENA is currently investigated within the European design study LAGUNA-LBNO. In LENA low energy neutrinos will be used as probes from astrophysical objects, like supernovae. The main goal of the Chinese JUNO project is the precise measurement of neutrino oscillation parameters with reactor neutrinos at a distance of about 60 km between source and detector. In the short baseline reactor experiment Double Chooz the third mixing angle  $\theta_{13}$  is going to be measured with high accuracy and Borexino is very successful in measuring low energy neutrinos from thermal fusion processes in the center of our Sun.

Two characteristics of proton recoils are of special interest. Firstly, the energy response of protons in liquid scintillators is strongly non-linear. This effect, commonly called quenching, has to be known to predict the energy scale of the appearing signals and backgrounds. Secondly, electron and proton recoils show a different scintillation pulse shape. This can be used for particle identification via pulse shape discrimination (PSD).

## Experimental setup

The CRESST/EURECA neutron scattering facility [5, 6] at the MLL tandem accelerator provides an optimal infrastructure to characterize different scintillator mixtures under neutron irradiation. A  $^{11}\text{B}$  beam is guided onto a gaseous  $\text{H}_2$ -target to obtain monoenergetic neutrons between about 6 – 11 MeV depending on the detector position with respect to the beam axis. Using a pulsed beam (pulse width about 2-3 ns (FWHM)) the neutron energy can be precisely determined by a Time-of-Flight measurement (ToF). In the scintillator the neutrons scatter off protons, which are then detected by their characteristic scintillation response.

The scintillation detector consists of a scintillator sample container (cylindric 3 inch by 1 inch PTFE box with a quartz-glass window) and a fast 3 inch photomultiplier tube (PMT), to detect the scintillation light. The PMT signal is recorded by a flash ADC (14 bit and 2 GHz sampling). This allows to study the pulse shape of the scintillation signal. To sample different neutron energies, the angle between the beam axis and the detector can be varied.

The setup has been improved in the scope of several Diploma, Master and two Ph.D. theses during beam times performed together with the CRESST group. Here results from a beam time in August 2012 are shown. In this beam time different LAB-based scintillators with different concentrations of the flours PPO and bisMSB were characterized. Also samples with an admixture of non-scintillating mineral oil have been investigated. To study degradation due to oxygen contamination two samples have been exposed to air for different amounts of time.

## Pulse-shape discrimination (PSD)

As the neutrons are slower than the  $\gamma$ s the neutron and the  $\gamma$ -events can be separated by ToF (see figure 1). Hence, clean samples of both event types can be selected. See figure 2 for an example of the resulting mean pulse shapes for neutron and  $\gamma$ -events. The pulse shapes of both event types can be characterized and the PSD capabilities of different scintillators mixtures can be compared.

To compare the PSD power of the scintillator samples the neutron selection efficiency  $\epsilon_n$  for a fixed  $\gamma$ -rejection of 99% was determined for 0.5 MeV energy intervals between

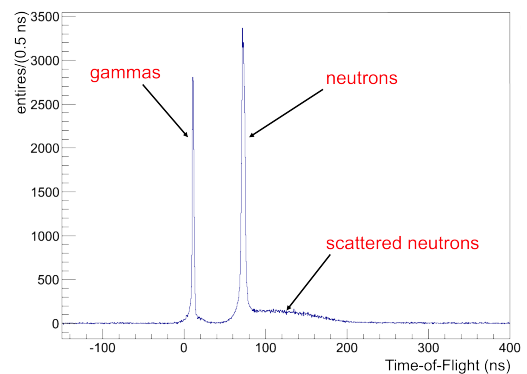


Figure 1: Time-of-Flight spectrum for neutrons with an energy of 10.8 MeV featuring two peaks: the  $\gamma$ -peak at a ToF of about 10 ns and the neutron peak at about 75 ns [7].

\* This research was supported by the DFG cluster of excellence 'Origin and Structure of the Universe' and by the European Community via the 'LAGUNA-LBNO - Design of a pan-European Infrastructure for Large Apparatus studying Grand Unification, Neutrino Astrophysics and Long Baseline Neutrino Oscillations' FP7 grant.

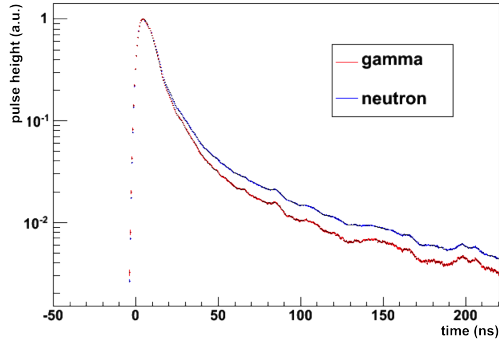


Figure 2: Mean pulses of neutrons (blue) and gammas (red) for LAB + 3 g/l PPO + 20 mg/l bisMSB [8].

0 and 5.5 MeV. For energies in the range 0-0.5 MeV,  $\epsilon_n$  was found to be in the range of 68.58%-85.96% depending on the liquid scintillator sample. For energies between 1-1.5 MeV,  $\epsilon_n$  ranges from 96.33%-99.82%. It was found that increasing the PPO concentration increases  $\epsilon_n$ , while replacing 50% of the LAB by non-scintillating mineral oil or exposing the sample to air reduces  $\epsilon_n$  [8].

### Proton quenching

To characterize the proton quenching, again the ToF is used to select a pure sample of proton recoils. Furthermore, the kinetic energy of the incident neutrons  $E_{\text{kin}}^n$  can be determined from the ToF. Since  $m_n \approx m_p$ , where  $m_n$  is the neutron and  $m_p$  the proton rest mass, the maximum proton recoil energy can be approximated to be  $E_{\text{max}}^p \approx E_{\text{kin}}^n$ . The maximum visible proton recoil energy  $E_{\text{max}}^{\text{vis}}$  is reconstructed from the obtained recoil spectrum recorded in up to eight detector positions (i.e. neutron energies). The visible energy scale is defined by calibration with  $\gamma$ -sources<sup>1</sup> [9]. Varying the angle of the detector w.r.t. to the beam axis,  $E_{\text{max}}^{\text{vis}}(E_{\text{max}}^p)$  can be determined. An example is shown in figure 3. The resulting data points are fitted with the semi-empiric quenching model of Birks [10], which models the quenching effect with two parameters: the light yield and the so called kB-factor.

A detailed proton quenching analysis is still in progress. Here only a preliminary result for LAB + 3 g/l PPO + 20 mg/l bisMSB is shown. The fit result for the kB-factor is  $(0.0143 \pm 0.003) \text{ cm MeV}^{-1}$  [7, 9, 11].

## REFERENCES

- [1] M. Wurm et al., *Astroparticle Physics*, Volume 35, Issue 11, p. 685-732 (2012)
- [2] Yifang Wang, private communication, JUNO (2013)
- [3] Double Chooz collaboration, Y. Abe et al., *Phys. Rev. D* 86, 052008 (2012)
- [4] Borexino collaboration, G. Alimonti et al., *Astropart.Phys.* 16 (2002) 205-234
- [5] C. Ciemiak, Ph.D. thesis, TU München, 2011

<sup>1</sup>Calibration sources used:  $^{22}\text{Na}$ ,  $^{137}\text{Cs}$ ,  $^{228}\text{Th}$ , AmBe

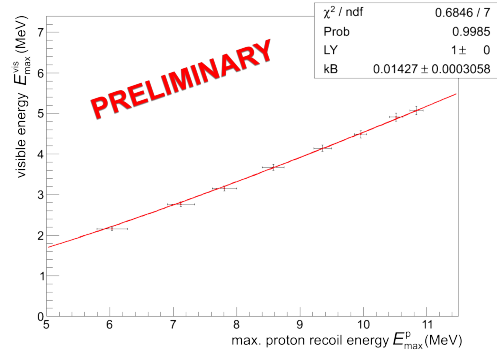


Figure 3: Reconstructed maximum visible proton recoil energy  $E_{\text{max}}^{\text{vis}}$  plotted versus the maximum proton recoil energy  $E_{\text{max}}^p \approx E_{\text{kin}}^n$ , determined by ToF. Data points fitted with Birks model and fixed light yield (LY) [7].

- [6] R. Strauß, Ph.D. thesis, TU München, 2013
- [7] V. Zimmer, Ph.D. thesis, TU München, in preparation
- [8] J. Winter, Ph.D. thesis, TU München, 2013
- [9] L. Prade, Diploma thesis, TU München, 2013
- [10] J.B. Birks: *The Theory and Practice of Scintillation Counting*, Pergamon Press, Oxford, 1964.
- [11] J. Scherzinger, Diploma thesis, TU München, 2012